

# X-Restormer++: 1st Place Solution for the UG2+ CVPR 2026 All-Weather Restoration Challenge

Youwei Pan Leilei Cao\* Yingfang Zhu Fengjie Zhu  
TEX AI, Transsion Holdings  
{youwei.pan, leilei.cao}@transsion.com

## Abstract

*In this work, we present our winning solution for the 8th UG2+ Challenge (CVPR 2026) Track 1: Image Restoration under All-weather Conditions. Our method is built upon the strong baseline framework X-Restormer, which effectively captures both channel-wise global dependencies and spatially-local structural information through its dual-attention design (Multi-DConv Head Transposed Attention and Overlapping Cross-Attention). To further boost the restoration performance, we propose several key improvements. First, we integrate the spatially-adaptive input scaling mechanism from Restormer-Plus to dynamically adjust the spatial weights of the input image, enhancing spatial adaptability. Second, to better preserve structural details and edge information, we introduce a novel Gradient-Guided Edge-Aware (GGEA) loss, which is combined with L1 and Multi-Scale SSIM losses in a unified training objective. Third, we significantly expand the training data by incorporating an extra 24,500 degraded-clean image pairs from FoundIR and WeatherBench alongside the original WeatherStream dataset. With these strategies, our proposed method successfully ranks the 1st place in the challenge.*

## 1. Introduction

Adverse weather conditions such as rain, snow, haze, and fog severely degrade the quality of outdoor images, posing significant challenges for downstream computer vision tasks including object detection, semantic segmentation, and autonomous driving. The 8th UG2+ Challenge (CVPR 2026) Track 1: Image Restoration under All-weather Conditions aims to develop robust methods that can handle diverse and complex weather degradations in real-world scenarios.

Image restoration under adverse weather is inherently challenging due to: (1) the diversity of degradation types that may co-occur in a single image; (2) the spatially vary-

ing nature of weather artifacts; and (3) the need to preserve fine structural details while removing degradation patterns. Traditional pixel-wise loss functions such as L1 or MSE treat all spatial locations equally, which often leads to over-smoothed results where edge and texture details are insufficiently recovered.

In this report, we present our state-of-the-art solution built upon the strong baseline framework X-Restormer [1]. The core of X-Restormer is a dual-attention design within each Transformer block, utilizing both Multi-DConv Head Transposed Attention (MDTA) and Overlapping Cross-Attention (OCA) to capture complementary global and local structural information.

To tackle the aforementioned challenges and push the performance limits, we introduce three major improvements over the base X-Restormer architecture: First, to improve the network’s spatial adaptability, we integrate the **spatially-adaptive input scaling mechanism inspired by Restormer-Plus** [8]. Instead of using a standard global additive residual connection, this mechanism dynamically predicts a spatial weight map to scale the input image before adding the network’s residual output, allowing for more precise detail retention in background regions. Second, we propose a novel **Gradient-Guided Edge-Aware (GGEA) Loss**. By exploiting the Sobel gradient map of the ground-truth image to construct a spatially adaptive weight map, the GGEA loss assigns higher importance to edge and high-frequency regions during training. This is combined with L1 and Multi-Scale SSIM losses to effectively guide the network in reconstructing critical structural details. Finally, to enhance the model’s generalization and robustness against diverse weather degradations, we significantly expand the scale of our training data. In addition to the original WeatherStream dataset, we incorporate an extra 24,500 degraded-clean image pairs provided by FoundIR [4] and the WeatherBench [3] dataset. With these architectural, objective, and data-level enhancements, our proposed method ranks 1st place in the 8th UG2+ Challenge (CVPR 2026) Track 1, achieving an outstanding PSNR of 29.1907 and an SSIM of 0.8341.

\* Corresponding author

## 2. Proposed Method

### 2.1. Overview and Network Architecture

Our model is built upon X-Restormer [1], and the overall pipeline is illustrated in Figure 1. Unlike the standard Restormer [6], X-Restormer integrates Overlapping Cross-Attention (OCA) [2] for local spatial interactions and we adopt a spatially-adaptive input scaling mechanism from Restormer-Plus [8] to dynamically adapt to non-uniform weather degradations. The detailed architecture of these components can refer to their respective papers. To further improve the restoration performance in this challenge, we propose several key strategies to enhance the model, including a novel Gradient-Guided Edge-Aware (GGEA) Loss and a composite data expansion strategy.

### 2.2. Gradient-Guided Edge-Aware (GGEA) Loss

In addition to the architectural improvements, we employ the Gradient-Guided Edge-Aware Loss, inspired by DiffBIR [5], which leverages the structural information from the ground-truth image to construct a spatially adaptive weight map for the reconstruction loss.

#### 2.2.1. Motivation

Standard pixel-wise losses (e.g., L1, MSE) assign equal importance to all spatial locations. However, in weather-degraded images, edge and texture regions are often the most severely affected and the most perceptually important. By explicitly guiding the network to focus on these high-frequency regions, we can achieve better structural fidelity in the restored images.

#### 2.2.2. Edge Weight Map Generation

Given a ground-truth image  $I_{\text{gt}} \in \mathbb{R}^{N \times 3 \times H \times W}$ , where  $N$  denotes the batch size, and  $H, W$  represent the spatial height and width respectively, the edge weight map is computed as follows:

##### Step 1: Grayscale Conversion.

$$I_{\text{gray}} = 0.2989 \cdot I_{\text{gt}}^R + 0.5870 \cdot I_{\text{gt}}^G + 0.1140 \cdot I_{\text{gt}}^B \quad (1)$$

where  $I_{\text{gt}}^R, I_{\text{gt}}^G$ , and  $I_{\text{gt}}^B$  denote the red, green, and blue color channels of the ground-truth image  $I_{\text{gt}}$ .

**Step 2: Sobel Gradient Computation.** We apply the horizontal and vertical Sobel operators, defined as:

$$G_x = \begin{bmatrix} 1 & 0 & -1 \\ 2 & 0 & -2 \\ 1 & 0 & -1 \end{bmatrix}, \quad G_y = \begin{bmatrix} 1 & 2 & 1 \\ 0 & 0 & 0 \\ -1 & -2 & -1 \end{bmatrix} \quad (2)$$

The gradient magnitude map  $M$  is computed as:

$$M = \sqrt{(I_{\text{gray}} * G_x)^2 + (I_{\text{gray}} * G_y)^2} \quad (3)$$

where  $*$  denotes the 2D convolution operation with replicate padding to maintain the spatial resolution.

##### Step 3: Block-wise Aggregation with tanh Activation.

To obtain a smooth and stable weight map, we partition the gradient magnitude map  $M$  into non-overlapping  $2 \times 2$  blocks and compute the block-wise sum:

$$B_{i,j} = \sum_{m=0}^1 \sum_{n=0}^1 M[2i+m, 2j+n] \quad (4)$$

where  $(i, j)$  are the spatial indices of the downsampled blocks, and  $(m, n)$  are the local offsets within each  $2 \times 2$  block. The tanh activation is then applied to normalize the block sums:

$$W_{i,j} = \tanh(B_{i,j}) \quad (5)$$

The resulting weight  $W_{i,j}$  is then replicated back to the original spatial resolution by repeating each block value across its corresponding  $2 \times 2$  region, yielding the full-resolution weight map  $W \in \mathbb{R}^{N \times 1 \times H \times W}$ .

The tanh activation serves two purposes: (1) it bounds the weight values to the range  $[0, 1]$ , preventing extreme gradients from dominating the loss; (2) it provides a smooth, differentiable mapping that preserves the relative ordering of edge strengths.

#### 2.2.3. Comparison with DiffBIR’s Weighted Loss

We further compare our GGEA loss with the weighted loss proposed in DiffBIR [5]. The key differences between the two approaches are:

- **Weight Map Source:** DiffBIR computes the weight map from the *predicted image* (output of the network during training), while our GGEA loss computes it from the *ground-truth image*.
- **Weight Map Formulation:** DiffBIR uses  $W = 1 - \tanh(B)$  where  $B$  is the block-wise gradient sum, effectively assigning lower weights to edge regions. In contrast, our method uses  $W = \tanh(B)$ , directly assigning higher weights to edge regions.
- **Error Metric:** DiffBIR uses squared error (MSE), while we use absolute error (L1) for better robustness to outliers.

#### 2.2.4. GGEA Loss Formulation

The final GGEA loss is defined as:

$$\mathcal{L}_{\text{GGEA}} = \frac{1}{N \cdot H \cdot W} \sum_{n,c,h,w} W_{n,h,w} \cdot |\hat{I}_{n,c,h,w} - I_{\text{gt},n,c,h,w}| \quad (6)$$

where  $\hat{I}$  is the restored image predicted by our network,  $W$  is the broadcasted edge weight map, and  $|\cdot|$  denotes the absolute value. The indices  $n, c, h, w$  iterate over the batch, channel, height, and width dimensions, respectively. Note that the weight map  $W$  is derived solely from the ground-truth image and is detached from the computational graph, ensuring stable training dynamics.

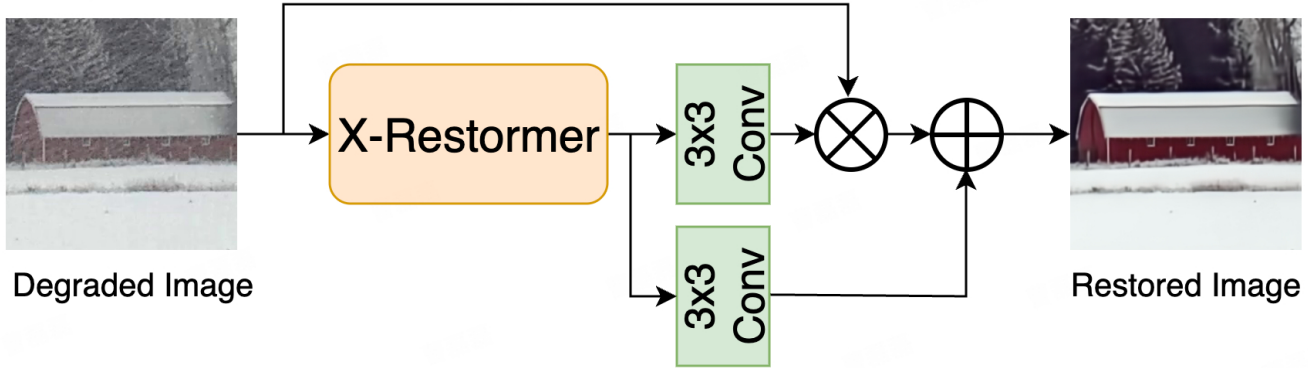


Figure 1. The overall framework of our proposed method.

### 2.3. Total Training Loss

The complete training loss combines three components:

$$\mathcal{L}_{\text{total}} = \mathcal{L}_{\text{L1}} + \lambda_{\text{ssim}} \cdot \mathcal{L}_{\text{MS-SSIM}} + \mathcal{L}_{\text{GGEA}} \quad (7)$$

where  $\lambda_{\text{ssim}} = 1.0$  is the balancing weight for the Multi-Scale SSIM loss. Each loss component serves a complementary role:

- $\mathcal{L}_{\text{L1}}$ : Provides stable pixel-wise supervision for overall reconstruction fidelity.
- $\mathcal{L}_{\text{MS-SSIM}}$ : Captures multi-scale structural similarity, encouraging perceptually consistent restoration.
- $\mathcal{L}_{\text{GGEA}}$ : Focuses the network on edge and texture regions, improving structural detail recovery.

## 3. Experiment Details

### 3.1. Dataset

Our training set comprises three datasets: 24,500 degraded-clean image pairs provided by FoundIR [4], WeatherBench [3], and the training set of WeatherStream [7].

### 3.2. Optimization

We optimize our model using AdamW with an initial learning rate of  $3 \times 10^{-4}$  and a weight decay of  $1 \times 10^{-4}$ . The learning rate is scheduled by cosine annealing, decaying to a minimum of  $1 \times 10^{-6}$  following a 1-epoch linear warmup. The base batch size is set to 18, and we apply gradient accumulation over 4 steps to achieve an effective batch size of 72. During the training phase, input images of varying resolutions are randomly cropped to a fixed patch size of  $128 \times 128$ . The entire training process spans 40 epochs and is conducted on a single NVIDIA H100 (80 GB) GPU. Additionally, the MS-SSIM kernel size is set to 7, which satisfies the spatial constraint  $\text{img\_size} \geq (\text{kernel\_size} - 1) \times 16 + 1$ .

Table 1. Quantitative comparison on the challenge test set. Our method (panyouwei) achieves the first place.

Rank	Team	PSNR (dB)	SSIM
1	<b>panyouwei (Ours)</b>	<b>29.1907</b>	<b>0.8341</b>
2	dakiet	28.1198	0.7859
3	y1nnng	25.3964	0.7797
4	openclaw	24.7583	0.7811
5	muzhou	24.1254	0.7588

### 3.3. Inference Strategy

During inference, We adopt the same multi-frame averaging strategy as Restormer-Plus [8]. For each scene containing multiple degraded observations, we independently process each degraded image through the trained model and compute the pixel-wise mean of all restored outputs. Input images are padded to be divisible by 8 using reflective padding, and the padding is removed after inference.

## 4. Main Results

### 4.1. Quantitative Results

Table 1 presents the quantitative comparison of the top-5 methods on the challenge leaderboard. Our method achieves the best performance among all participating teams.

Our method outperforms the second-place method by **1.07 dB** in PSNR and **0.0482** in SSIM. Compared to the third-place method, our approach achieves a significant improvement of **3.79 dB** in PSNR, highlighting the substantial performance gap between our method and other competitive solutions.

### 4.2. Qualitative Results

Figure 2 and Figure 3 show qualitative comparisons on challenging weather-degraded scenes. We select representative

scenes with diverse and complex degradation patterns to demonstrate the effectiveness of our method.

As shown in Figure 2 and Figure 3, we present results on 8 challenging scenes with diverse weather degradations. For each scene, we show the degraded input image (marked with “degraded” suffix) and our restored output (marked with “restored” suffix). Our method effectively removes these diverse weather degradations while preserving fine structural details and textures. Notably, edge regions and texture details are well preserved thanks to the Gradient-Guided Edge-Aware loss, which guides the network to focus on high-frequency regions during training.

## 5. Ablation Results

### 5.1. Effectiveness of the Learnable Residual Scaling

To verify the effectiveness of the spatially-adaptive input scaling mechanism adopted from Restormer-Plus, we conduct an ablation study comparing the base version and the plus version of our network architecture.

Specifically, the two variants are implemented as follows:

- **Base Version:** Employs a standard global additive residual connection. The final restored image is obtained by simply adding the network’s predicted residual map to the degraded input image.
- **Plus Version (Ours):** Introduces a dynamic skip connection. The network predicts an additional spatial weight map via a  $3 \times 3$  convolution to dynamically modulate the input image before adding the residual features.

The quantitative comparison is presented in Table 2. As shown in the results, the Plus version consistently outperforms the Base version in terms of both PSNR and SSIM. This improvement demonstrates that the dynamic skip connection provides greater flexibility. Instead of treating all spatial locations equally, it allows the network to adaptively decide how much original image information to retain, which is particularly crucial for handling complex, non-uniform weather degradations and preserving background structural details.

Table 2. Ablation study on the residual scaling mechanism. The Plus version yields better restoration performance.

Model Variant	PSNR $\uparrow$	SSIM $\uparrow$
X-Restormer (Base)	28.9617	0.8178
X-Restormer (Plus)	<b>29.1907</b>	<b>0.8341</b>

### 5.2. Comparison with X-Restormer without GGEA Loss

We first compare our method with the X-Restormer trained using only L1 and MS-SSIM losses. As shown in Table 3,

Table 3. Ablation study on the effectiveness of GGEA Loss. Both models are trained for 40 epochs with identical data augmentation and optimization settings.

Loss Configuration	PSNR (dB)	SSIM
L1 + MS-SSIM	28.9222	0.8123
L1 + MS-SSIM + GGEA Loss (Ours)	<b>29.1907</b>	<b>0.8341</b>

Table 4. Comparison with DiffBIR’s weighted loss on the test set. All models are trained with the same backbone architecture and training settings.

Loss Configuration	PSNR (dB)	SSIM
L1 + MS-SSIM + DiffBIR Weighted Loss	29.0651	0.8219
L1 + MS-SSIM + GGEA Loss (Ours)	<b>29.1907</b>	<b>0.8341</b>

the addition of GGEA loss brings consistent improvements across different metrics.

The GGEA loss provides a PSNR improvement of **0.2685 dB**. While the SSIM shows a marginal decrease of **0.0218**. The PSNR gain indicates improved pixel-level fidelity, particularly in edge and texture regions where the gradient-guided weighting focuses the network’s attention.

### 5.3. Comparison with DiffBIR’s Weighted Loss

Our GGEA loss outperforms DiffBIR’s [5] weighted loss by **0.1256 dB** in PSNR, which are presented in Table 4. The superiority of our approach can be attributed to two factors:

**1. Ground-Truth Based Weight Map:** Using the ground-truth image to generate the weight map provides a stable and accurate spatial prior during training. In contrast, DiffBIR’s approach of using the predicted image introduces instability, as the weight map changes dynamically during training and may not accurately reflect the true edge distribution.

**2. Direct Edge Emphasis:** Our formulation  $W = \tanh(B)$  directly assigns higher weights to edge regions, encouraging the network to focus on reconstructing high-frequency details. DiffBIR’s formulation  $W = 1 - \tanh(B)$  inverts this relationship, which may inadvertently de-emphasize the very regions that require the most attention in image restoration tasks.

### 5.4. Analysis of Weight Map Design Choices in GGEA Loss

We provide a detailed breakdown of the design choices in Table 5. We compare our design against an alternative that derives the weight map from the predicted image with an inverted formulation  $W = 1 - \tanh(B)$ , which suppresses edge regions during loss computation. In contrast, our design computes the weight map from the ground-truth and adopts  $W = \tanh(B)$  to directly assign higher weights to edge regions. The results show that our formulation yields a



Figure 2. Qualitative results on challenging scenes (Part 1). Each scene shows the degraded input and our restored output.



Figure 3. Qualitative results on challenging scenes (Part 2). Each scene shows the degraded input and our restored output.

notable improvement of **0.2631 dB** in PSNR and **0.0239** in SSIM, confirming that both deriving the weight map from the ground-truth and explicitly emphasizing edge regions are essential for the final performance gain.

### 5.5. Effect of Multi-Frame Averaging Strategy

During inference, we compare two strategies for handling scenes with multiple degraded observations:

- **Single-Frame Inference:** Each degraded image is pro-

Table 5. Ablation study on weight map design choices.

Weight Source	Weight Formula	PSNR (dB)	SSIM
Predicted Image	$W = 1 - \tanh(B)$	28.9276	0.8102
Ground-Truth	$W = \tanh(B)$ (Ours)	<b>29.1907</b>	<b>0.8341</b>

Table 6. Comparison of inference strategies on the validation set.

Inference Strategy	PSNR (dB)	SSIM
Single-Frame Inference	29.0001	0.8288
Multi-Frame Averaging	<b>29.1907</b>	<b>0.8341</b>

cessed independently, and the PSNR/SSIM is computed for each output separately. The final metric for a scene is the average of all individual frame metrics.

- **Multi-Frame Averaging:** All degraded images in a scene are processed independently, and the outputs are averaged pixel-wise to produce a single restored image. The metric is computed between this averaged output and the ground truth.

The results are presented in Table 6. The multi-frame averaging strategy outperforms single-frame inference by **0.1906 dB** in PSNR and **0.0053** in SSIM. The improvement can be attributed to several factors:

- **Noise Reduction:** Averaging multiple predictions reduces random noise and artifacts that may appear in individual restorations. Since weather degradations (rain streaks, snowflakes) are often spatially varying across frames, their artifacts tend to cancel out during averaging.
- **Complementary Information Fusion:** Different degraded images of the same scene capture complementary information due to temporal variations in weather patterns. For instance, rain streaks may appear at different spatial locations in different frames, and averaging effectively fuses this complementary information.
- **Robustness to Frame-Specific Degradations:** Some frames may suffer from more severe degradations than others. Multi-frame averaging mitigates the impact of heavily degraded frames by incorporating information from cleaner frames.

## 5.6. Effect of Training Data Scale

To investigate the impact of training data scale on model performance, we conduct experiments with increasing the training dataset size. The results are presented in Table 7. The experimental results demonstrate that expanding the training dataset yields consistent performance improvements.

The final training set comprises three datasets: training set from WeatherStream [7], WeatherBench [3], and

Table 7. Ablation study on training data scale. All models are trained for 40 epochs with the same architecture and training settings.

Training Dataset	PSNR (dB)	SSIM
WeatherStream	28.0314	0.7851
WeatherStream + WeatherBench + FoundIR	<b>29.1907</b>	<b>0.8341</b>

24,500 degraded-clean pairs from FoundIR [4]. This diverse dataset covers a wide range of weather conditions including rain, snow, fog, and haze, enabling the model to learn robust representations for multi-weather image restoration.

## 6. Conclusion

In this paper, we presented our winning solution for the 8th UG2+ Challenge (CVPR 2026) Track 1: Image Restoration under All-weather Conditions. Built upon the strong baseline framework X-Restormer, we introduce three key improvements: spatially-adaptive input scaling mechanism, Gradient-Guided Edge-Aware loss, and expanded training data with additional 24,500 image pairs from FoundIR and WeatherBench. Our method achieves a PSNR of 29.1907 dB and SSIM of 0.8341 on the testing set, ranking 1st place in the challenge.

## References

- [1] Xiangyu Chen, Zheyuan Li, Yuandong Pu, Yihao Liu, Jiantao Zhou, Yu Qiao, and Chao Dong. A comparative study of image restoration networks for general backbone network design. *arXiv preprint arXiv:2310.11881*, 2023. 1, 2
- [2] Xiangyu Chen, Xintao Wang, Jiantao Zhou, Yu Qiao, and Chao Dong. Activating more pixels in image super-resolution transformer. In *Proceedings of the IEEE/CVF conference on computer vision and pattern recognition*, pages 22367–22377, 2023. 2
- [3] Qiyuan Guan, Qianfeng Yang, Xiang Chen, Tianyu Song, Guiyue Jin, and Jiyu Jin. Weatherbench: A real-world benchmark dataset for all-in-one adverse weather image restoration. In *Proceedings of the 33rd ACM international conference on multimedia*, pages 12607–12613, 2025. 1, 3, 6
- [4] Hao Li, Xiang Chen, Jiangxin Dong, Jinhui Tang, and Jinshan Pan. Foundir: Unleashing million-scale training data to advance foundation models for image restoration. In *Proceedings of the IEEE/CVF international conference on computer vision*, pages 12626–12636, 2025. 1, 3, 6
- [5] Xinqi Lin, Jingwen He, Ziyang Chen, Zhaoyang Lyu, Bo Dai, Fanghua Yu, Yu Qiao, Wanli Ouyang, and Chao Dong. Diffbir: Toward blind image restoration with generative diffusion prior. In *European conference on computer vision*, pages 430–448. Springer, 2024. 2, 4
- [6] Syed Waqas Zamir, Aditya Arora, Salman Khan, Munawar Hayat, Fahad Shahbaz Khan, and Ming-Hsuan Yang. Restormer: Efficient transformer for high-resolution image

restoration. In *Proceedings of the IEEE/CVF conference on computer vision and pattern recognition*, pages 5728–5739, 2022. [2](#)

- [7] Howard Zhang, Yunhao Ba, Ethan Yang, Varan Mehra, Blake Gella, Akira Suzuki, Arnold Pfahnl, Chethan Chinder Chandrappa, Alex Wong, and Achuta Kadambi. Weatherstream: Light transport automation of single image deweathering. In *Proceedings of the IEEE/CVF conference on computer vision and pattern recognition*, pages 13499–13509, 2023. [3](#), [6](#)
- [8] Chaochao Zheng, Luping Wang, and Bin Liu. Restormer-plus for real world image deraining: One state-of-the-art solution to the gt-rain challenge (cvpr 2023 ug2+ track 3). *arXiv preprint arXiv:2305.05454*, 2023. [1](#), [2](#), [3](#)